Electron Trajectory Simulation in Experimental Hall Thruster Fields

IEPC-2011-243

Presented at the 32nd International Electric Propulsion Conference,
Wiesbaden, Germany
September 11–15, 2011

Michael S. McDonald* and Alec D. Gallimore†
Plasmadynamics and Electric Propulsion Laboratory (PEPL)
University of Michigan, Ann Arbor, MI USA

The correct approach to electron transport modeling in Hall thrusters is an open question in the field and is compounded by a lack of comparative studies on the relative influence of various proposed electron transport mechanisms in the thruster plume. Lacking an analytical model for transport, empirical coefficients are used in most models to reproduce major discharge parameters like the total discharge current and thrust, and these models are then used to gain insight into less observable quantities, especially lifetime-limiting discharge channel erosion. As part of an ongoing comparative investigation of electron transport mechanisms in the H6 6-kW Hall thruster, we examine drift and collisional electron transport in the near field between the centrally mounted cathode and the discharge channel exit plane using Monte Carlo-type electron trajectory simulations and focusing on binary plume collisions and thruster surface interactions. Experimental measurements of the time-averaged electric field and neutral density are used as model inputs. Approximately 10^4 electrons are seeded from a Maxwellian energy distribution and their trajectories are numerically integrated. Drift and collisional transport mechanisms in the static fields are found insufficient to explain any transport from the centrally mounted cathode to the discharge channel exit plane, as expected. This null result is presented to discuss the modeling technique of direct electron trajectory integration and to motivate its extension to time-resolved fields in the near future, taking into account turbulent transport mechanisms.

I. Introduction: Electron Transport in Hall Thrusters

The electron trajectory model presented in this paper, dubbed 'MCHall', is designed to focus on the near-field plume, a region where large anomalous transport coefficients are imposed in current hybrid-PIC models. Several current trends in Hall thruster development motivate the development of more fully predictive thruster models. A brief review of Hall thruster electron modeling techniques and selected work to date and further motivation for MCHall and the near-field plume focus are given in Section II. A detailed discussion of the formulation of MCHall is given in Section III. Ultimately MCHall is intended for application to planned time-resolved plume maps of plasma potential and density in the H6 near-field. Since this data is not yet available, we examine here a realistic distribution of electrons simulated seeded from a point-source cathode into static experimental fields as a baseline test in Section IV.

A. The motivation for improved models

The Hall thruster is a mature space flight technology in the 1600-3000 second specific impulse range, with peak flight power levels demonstrated at 4.5 kW to date on the BPT-4000 and ground units tested with nominal power levels up to 50 kW. However, despite this high level of maturity and long flight heritage, computer models of the device remain relatively primitive and a large part of thruster development to date has been heavily experimental in nature. This empirical approach will become increasingly unsustainable in the coming years due to several factors.

*Doctoral Candidate, University of Michigan, Applied Physics Program. msmcdon@umich.edu.
†Arthur F. Thurnau Professor, Department of Aerospace Engineering. Director of the Plasmadynamics and Electric Propulsion Laboratory. alec.gallimore@umich.edu.

First, while Hall thrusters are traditionally thought of as devices well-suited to a specific impulse range from 1600-3000 seconds, efforts are underway to widen this specific impulse in both directions, for higher thrust-to-power at low specific impulses near 1000 seconds and increased total thruster efficiency at very high specific impulses approaching 4000 seconds. Practically this means driving the thruster to very low and high voltage extremes, which on the high end raises concerns due to elevated discharge channel erosion at high voltage[1] and on the low end brings challenges due to unstable thruster operation below a threshold of around 100 V.

In addition to efforts to better optimize thruster performance at a given power level by expanding the I_{sp} envelope, the overall power level of Hall thrusters is also growing. Available space power has grown with advances in solar technology, doubling approximately every four years over the last five decades in a Moore's Law type exponential curve according to Brophy[2], and thruster development is following: several thrusters in the 10-40 kW range are currently under development or active testing including the NASA 300M, 400M and 457M and the Busek BHT-20K,[3–6] and further units up to 200 kW are on the drawing board.[7] With increased power comes facility-level challenges as vacuum chambers capable of maintaining acceptably high vacuum at xenon mass flow rates on the order of 100 mg/sec for 100 A discharge currents are few. Scarcity of testing locations aside, consumable resources are a considerable expense both for xenon propellant and liquid nitrogen for cryopump cooling and these costs are already motivating the increasing use of xenon recovery systems and the development of more efficient cryocooling systems.

Increased power also increases thruster size, given the typical annular channel shape and upper limits to the current density range where Hall thrusters operate well. Limits to discharge current density also necessarily reduce thrust density. The large physical footprint and sheer manufacturing difficulties of very high-power Hall thrusters makes the single annular channel Hall thruster difficult to scale past 100 kW, while projected throttling and other performance advantages have driven the development of the nested Hall thruster concept with two or three concentric Hall thrusters in a single package.[7,8] Modeling a Hall thruster with a single channel is already challenging; multiple channels guarantee a more complicated magnetic circuit and may give rise to inter-channel interactions or unstable cathode coupling between several discharges simultaneously, increasing the complexity linearly at best, exponentially at worst.

These factors motivate continued refinement of thruster models to achieve greater predictive capability and allow rapidly iterative thruster design, with less of the extensive and expensive ground testing and validation of new thruster concepts necessary today. Ideally a Hall thruster model would someday be able to perform parametric studies of the thruster design space by computer simulation before the first iron is cut or magnet coil is wound. This capability is still distant, but even small improvements to predictive modeling capabilities can have a valuable impact on Hall thruster development costs.

B. The electron transport problem

In a Hall thruster discharge the majority of electrons that leave the cathode orifice exit into the far-field plume to neutralize the accelerated ion beam. The remainder couple into the main discharge in the thruster channel and near-field plume, where they sustain the plasma through an ionization cascade in the injected neutral propellant. In practice, so-called "backstreaming" electron current from the cathode to the anode constitutes the largest loss mechanism in modern Hall thrusters, making up on the order of 20% of the discharge current even in highly efficient thrusters. This fraction is evaluated by comparing the total ion beam current in integrated Faraday probe sweeps of the thruster plume to the measured discharge current at the power supply. The difference is the electron current. These 20% of electrons are the focus of the electron transport debate.

A naive picture of an ideal Hall thruster might be to imagine a discharge sustained by a single "golden electron" emitted from the cathode toward the anode, triggering an ionization cascade and sustaining the discharge in perpetuity while the remainder of the cathode-born electrons exit to the thruster far field to neutralize the ion beam. Such a configuration would have a current utilization efficiency of unity, but this picture is too simple; the influence of backstreaming electron current on thruster operation is not black and white. To see why, consider an electron emitted in a 300 V discharge in xenon, with an ionization potential of approximately 12 eV. In a best-case scenario if the electron ionized neutrals repeatedly as it fell through the discharge potential, it would have enough energy to create 25 ions expending 12 eV of energy each time before reaching 300 V. If each ionization-born electron did the same, a single electron could produce a large (2^{25} or ~10^{10}), but not infinite, number of electrons to sustain the discharge. Thus, even in principle the golden electron is not enough and some fraction (however small) of cathode-born electrons are continuously required to sustain the discharge.

As noted above the real fraction of backstreaming electron current is much larger, not the 1 in 2^{25} of this implausible scenario but in fact more like the 1 in 4 or 5. This is because each electron does not create an ion each time it acquires

exactly one ionization potential's worth of energy – in fact, the ionization cross-section is about 10 times larger at 30 eV than it is at the 12 eV threshold. Some electrons will not produce any ions at all, some electrons lose energy in inelastic excitation collisions with neutrals, some energy is expended in self-heating of the cathode insert through ion bombardment to maintain thermionic emission, some energy is deposited into the anode by electrons arriving with non-zero temperature, some energy is deposited into the insulating walls in the discharge channel, and many other loss mechanisms besides. Nevertheless, there is a fundamental limit on the beam current fraction achievable at a given discharge voltage, and it is important to remember that some amount of backstreaming electron current is required for a thruster to operate. From an efficiency standpoint, it is desirable to make that fraction as small as possible while maintaining discharge stability.

With their small mass, electrons in the Hall thruster plume ought to be tightly confined along magnetic ($\boldsymbol{B}$) field lines, even when an electric ($\boldsymbol{E}$) field is applied to drive them across the magnetic field. In the archetypal picture of the Hall thruster with uniform axial electric and radial magnetic fields, this plays out as the well-known $\boldsymbol{E} \times \boldsymbol{B}$ drift, with incremental transport across $\boldsymbol{B}$ in the direction of $\boldsymbol{E}$ permitted with electron-neutral or electron-ion collisions. In the real thruster, the $\boldsymbol{E} \times \boldsymbol{B}$ drift takes on a far more complex shape, but the physical principle of cross-field transport via collisions still holds. However, as early as the 1960s Janes found this mechanism, the so-called "classical" transport due to binary collisions with heavy particles, to be orders of magnitude too small to account for experimentally observed cross-field currents in Hall thrusters.[9] This deficit is still observed today, and a wide variety of transport mechanisms have been proposed for the unexplained electron passage through the thruster plume.

These mechanisms are broadly classified into two types, collisional and turbulent transport. Collisional transport follows the same logic as the classical transport outlined above, but with the important caveat that the entire thruster is itself a body capable of colliding with electrons and inducing cross-field transport. In the discharge channel this mechanism is called near-wall conductivity and was first proposed by Morozov in the early Russian development of the stationary plasma thruster (SPT).[10,11] However, collisional transport is not limited to the discharge channel. In the thruster near field the inner magnet forms a magnetic mirror encouraging electron bouncing across the discharge channel between the thruster poles, and the interaction of the electrons with the thruster pole surfaces may also play a role. This mechanism has been explored previously in electron trajectory simulations by Smith, and inspired the development of MCHall.[12]

Turbulent transport is a proposed mechanism whereby induced azimuthal electric field components in the Hall thruster plasma create axial $\boldsymbol{E} \times \boldsymbol{B}$ drift components, such that electrons may engage in collisionless axial transport across the applied magnetic fields to the anode. Such field fluctuations are commonly attributed to plasma instabilities across a wide range of frequencies, ranging from the low single kilohertz up to several megahertz, with driving mechanisms including Rayleigh-Taylor or Kelvin-Helmholtz type effects, resonant interaction with characteristic electron or ion oscillations such as the upper or lower hybrid modes, ionization or other resistive instabilities, and others. Turbulent transport can be either coherent, corresponding to organized wave structures propagating in the plasma, or else decoherent, associated with random correlated fluctuations in the plasma potential and density.

II. Background: A history and overview of Hall thruster modeling techniques

Prior to the 1990s Hall thruster modeling was largely a theoretical affair. Owing to their near-exclusive development of the technology since 1970, a large part of the early analytical work on governing mechanisms in Hall thrusters was carried out in the former Soviet Union. Most of the analytical studies of this early period are 1D in the axial dimension of the thruster; treatment of the thruster in 2D or 3D did not begin until the rise of numerical simulation in the 1990s. We attempt here a brief overview of Hall thruster numerical modeling techniques, but while we list several works as examples this is not an exhaustive review.

A. Hybrid-Particle in Cell (PIC) Models

The first 2D models of the Hall thruster were hybrid-PIC treatments, leveraging the difference in mass between electrons and ions to treat the electrons as a continuous fluid, while the ions are treated as discrete particles (or, more commonly, superparticles representing millions or billions of ions). While not the first such model, one of the most well-known is Fife's HPHall, a 2D hybrid-PIC code in the axial and radial ($z - r$) directions.[13] Strictly speaking HPHall was not fully 2D, since it did not treat the radial direction as an independent coordinate. Instead the radial gridlines were mapped to magnetic field streamlines, and the electron fluid was treated using a 1D axial energy equation assuming isothermal electrons on the "radial" magnetic field lines. Since the magnetic field lines are only

approximately radial in a narrow region near the thruster exit plane corresponding to the Hall current and ionization / acceleration regions, the model's ability to reproduce physics outside of this band is hampered. Nevertheless, HPHall was one of the first modeling efforts to numerically reproduce the dominant Hall thruster "breathing mode" oscillation as a predator-prey cycle in the electron and neutral densities, along with the work of Boeuf.[14,15]

Electron mobility is not calculated from first principles in these models, instead it is empirically applied as due to one or both of two mechanisms: collisional wall transport in the Hall thruster channel and Bohm diffusion in the near-field plume due to azimuthal waves or turbulence of unknown origin. The mobility is defined as

$$\mu = \frac{e}{\nu_e m_e} \frac{1}{1 + (\omega_c/\nu_e)^2}$$

where ν_e is the electron collision frequency, ω_c is the cyclotron frequency and the other symbols have their usual meaning. Since classical collisions (e.g., electron-neutral and electron-ion collisions) are insufficient on their own, a new effective collision frequency is defined as a vehicle to introduce the various anomalous transport mechanisms. In the most general case an effective electron collision frequency $\nu_{e,eff}$ may be given as the sum of contributions due to classical collisions, wall collisions, and Bohm collisionality[16] as

$$\nu_{e,eff} = \nu_{e-n} + \nu_{e-wall} + \nu_{Bohm} = k n_n + a \times 10^7 + \frac{\alpha_B}{16}\omega_c \tag{1}$$

where k, a and α_B are constants and n_n is the neutral density. Fife initially used classical neutral collisions and Bohm collisionality alone, with a uniform value for $\alpha_B = 0.15$ over the whole simulation domain. Hagelaar[17] and later Koo[18] used a two-region mixed mobility model, with various strengths of Bohm collisionality in the near-field outside the discharge channel and wall collisions inside the discharge channel. Most recently Hofer used 3 regions with Bohm mobility alone in the updated version HPHall-2, with the three regions corresponding to the near-anode region, the ionization / acceleration zone, and the near-field.[19] All these methods discretize the true plasma behavior, where the level of electron mobility varies both spatially and temporally throughout the plume. These spatially discretized models require the largest introduction of anomalous transport in the near-field bridging the cathode to the thruster exit plane. Hofer describes this near-field region in HPHall as "*overlooked in the literature and [deserving of] significantly more scrutiny.*"

Most hybrid-PIC Hall thruster models are $z - r$ models, enabling convenient treatment of wall effects in the discharge channel radial boundary conditions. One unfortunate side-effect of this coordinate choice is that the azimuthal Hall current that lends the thruster its name and forms such a critical part of the thruster operation is not included in the model physics. Fernandez has created a z-theta model that notably does not introduce anomalous transport coefficients.[20] The simulation naturally develops a Hall current in the azimuthal direction, and azimuthal instabilities of the type theorized to drive turbulent cross-field transport form after electrons ionize background neutral gas. However, the model is not yet sufficiently stable to draw strong conclusions about electron transport mechanisms.

B. Kinetic simulations

Kinetic codes directly model both electrons and ions as discrete particles acted on by self-consistent electromagnetic forces. The large mass difference between electrons and ions hinders collisional energy transfer between the species, driving distinct energy levels with $T_e \gg T_i$. The electron velocities so greatly exceed the ions' that to simulate them individually requires much finer timescales than in hybrid-PIC modeling, but with advances in computing power kinetic simulations have grown more frequent.

Early kinetic codes relied on clever introduction of nonphysical electron/ion mass ratios or other rescaling of fundamental equations to sidestep the timescale problem. The first kinetic simulation of a Hall thruster with a true mass ratio was by Adam, et. al. in 2004.[21] This $z-\theta$ simulation code was notable for its reproduction of plausible cross-field electron transport without any anomalous transport coefficients over 100 μsec, after a full month of simulation time on a quad-core processor. Adam's results indicated a high-frequency short-wavelength instability in the discharge channel as a culprit for transport. An instability in this frequency and spatial range has since been detected experimentally,[22] though a direct experimental link correlating electron density and plasma potential in the instability has not yet been shown. Indeed, this may not be possible given the very high frequencies and short wavelengths of the instability.

C. Direct simulation of electron motion

MCHall belongs to a third category, the direct numerical integration of electron trajectories in imposed electric and magnetic fields. The first such code for Hall thrusters to the author's knowledge was by Smith, who in 2006 began work on a trajectory integrator for use with the Stanford Hall thruster.[12,23,24] Smith's work used static electric fields from a hybrid-PIC model as fixed inputs and simulated large ensembles of electrons from an energy and spatial distribution to generate bulk measurements in the plume and examine electron drift transport. The main finding of this vein of work was that collisions with thruster surfaces could drive a substantial amount of cross-field current to the discharge channel in the near-field, even in static, time-averaged fields devoid of turbulent transport. The work of Smith was a primary influence in developing MCHall.

Perez-Luna developed a similar approach in 2007, also using electric fields generated from a hybrid model. While Smith's focus was on collisional transport with thruster surfaces, Perez-Luna focused on turbulence, inspired in part by the success of Adam's kinetic treatment of the Hall thruster channel. In the static hybrid-PIC modeled fields the usual magnetic barrier to cross-field transport was observed, but when Perez-Luna introduced a simulated azimuthal wave based on the instability presented by Adam, collisionless cross-field transport at a velocity comparable to experimental estimates was observed.

If the main limitation of hybrid-PIC simulations are the necessity of anomalous coefficients fluid electron description, and the main limits of kinetic simulations are the massive computational costs, the limit of this type of simulation is that it is not self-consistent. Electrons are simulated completely in parallel, with no interaction with one another and with no opportunity to induce any changes in the static fields. As a result, electron trajectory integration can only treat turbulent transport mechanisms when the turbulent field is explicitly imposed. In this work MCHall will only be amine collisional transport, pending time-resolved mapping of the H6 Hall thruster plume.

All of these codes have been used to investigate anomalous electron transport mechanisms in the thruster plasma. The use of fields generated from hybrid codes is a cause for concern in both Smith's and Perez-Luna's work, since these codes generate fields using anomalous transport coefficients. Thus, the fields created are based on matching the overall discharge current or thrust, not on reproducing the actual plasma potential profiles, and may be biased to introduce nonphysical forms of electron mobility in the electron trajectory results. Only one brief work to date that we are aware of, by Alman[25], has actually simulated electron trajectories in experimentally measured thruster fields.

D. MCHall Motivation

MCHall was motivated by several factors. First, the results of Smith that cross-field transport even in the near-field plume could be explained in whole or in part by thruster surface collisions was an intriguing one, and the authors wished to use similar methods on a high-power, highly efficient Hall thruster with a centrally mounted cathode to see if the results could be reproduced and/or extended. Second, the model is intended for use with upcoming time-resolved maps of the H6 plume to evaluate turbulent transport in the H6 near-field, building on the pioneering work of Lobbia's high-speed Langmuir probe measurements of the BHT-600.[26,27]

The H6 Hall thruster is already the focus of experimental investigations of turbulent transport in the near-field due to rotating spoke instabilities,[28,29] and it is hoped that MCHall will be a vehicle for relative comparisons of transport by different methods in the near-field. Such a comparison might consider three cases: collisional-only transport in time-averaged fields, turbulent-only transport in time-resolved fields with thruster collisions disabled, and finally mixed transport with both time-resolved fields and thruster collisions enabled. Ultimately the solution to the electron transport problem is likely a combination of mechanisms in different plume regions and at different operating conditions, but experimentally these mechanisms are difficult and perhaps impossible to isolate, so modeling seems a prudent course of action if only to build intuition for future experimental investigations. At this point only collisional transport in time-averaged fields is considered.

III. Model Description

The model presented in this paper is essentially an integrator for the electron equations of motion in the plume of the H6 Hall thruster. The H6 Hall thruster is a nominal 6-kW class Hall thruster with a design operating condition at 300 V discharge voltage and 20 mg/s anode flow rate with a 7% cathode flow fraction. This thruster has been widely documented elsewhere, for example by Reid,[30–32] and is notable for its high anode efficiency, 64% at nominal 6-kW operation at 300V and 70% total efficiency at 6-kW 700V operation.[33] Since electron collisions are treated in a Monte

Carlo fashion the model is dubbed "MCHall", in a nod to the well-known HPHall simulation code. Wherever possible, MCHall model inputs have been guided by experimental measurements rather than appeal to the output of hybrid or other thruster modeling codes. The electric fields and neutral density are static and based on experimental measurements by Jameson at the nominal thruster operating condition,[34] and the electrons are sourced with a Maxwellian temperature based on experimental measurements in a hollow cathode similar to the one in the H6.[35]

A. Electron Trajectory Integration

The particle mover is the *sine qua non* of an electron trajectory simulator. Without an effective integrator for the electron equations of motion the electrons will be prone to numerical heating, requiring such short timesteps that simulation times become prohibitively long for reasonable numbers of electrons. For this work the leapfrog Boris algorithm with an adaptive timestep equal to a constant fraction of the local cyclotron frequency $\omega_c \Delta t = 10^{-3}$ is used. Since MCHall is written in MATLAB, a vector-based implementation of the algorithm is implemented following the development in Birdsall.[36]

The trajectory of a single electron is tracked through the Hall thruster plume by integrating the differential equations of motion. These equations are

$$\boldsymbol{a}(t) = -\frac{e}{m}\left(\boldsymbol{E} + \boldsymbol{v} \times \boldsymbol{B}\right) \tag{2}$$

$$\boldsymbol{v}(t) = \frac{d\boldsymbol{r}}{dt} \tag{3}$$

where e is the fundamental unit of charge, and the negative sign represents the negative charge of the electron. MCHall integrates these equations with a staggered leapfrog scheme. Given the position $\boldsymbol{r}$ at time t and a desired timestep Δt, the position at time $t + \Delta t$ is approximated by means of an intermediate velocity $\boldsymbol{v}$ at time $t + \Delta t/2$ as

$$\boldsymbol{r}_{t+\Delta t} = \boldsymbol{r}_t + \boldsymbol{v}_{t+\Delta t/2}\Delta t \tag{4}$$

$$\boldsymbol{v}_{t+\Delta t/2} = \boldsymbol{v}_{t-\Delta t/2} - \frac{e}{m}\left(\boldsymbol{E} + \boldsymbol{v}_t \times \boldsymbol{B}\right)\Delta t \tag{5}$$

where for compactness we define $\boldsymbol{r_t} \equiv \boldsymbol{r}(t)$. Evaluation of $\boldsymbol{v}_{t+\Delta t/2}$ in Eqn. (5) requires some subtlety due to the inclusion of $\boldsymbol{v}_t$ in the Lorentz force term. The simplifying insight first suggested by Buneman is to approximate the velocity symmetrically about the current time as

$$\boldsymbol{v}_t \approx \frac{\boldsymbol{v}_{t+\Delta t/2} + \boldsymbol{v}_{t-\Delta t/2}}{2} \tag{6}$$

This method maintains time reversibility of the model, a property discussed in more detail by Buneman. The use of an adaptive timestep (i.e., Δt is not constant) has not been found to introduce errors. Substitution in Eqn. (5) yields the implicit expression

$$\boldsymbol{v}_{t+\Delta t/2} = \boldsymbol{v}_{t-\Delta t/2} - \frac{e\Delta t}{m}\left(\boldsymbol{E} + \frac{1}{2}\left(\boldsymbol{v}_{t-\Delta t/2} + \boldsymbol{v}_{t+\Delta t/2}\right) \times \boldsymbol{B}\right) \tag{7}$$

The above equation can be solved directly via the component equations or in a matrix equation, as in the original work of Smith[37]; however, following the technique of Boris, we introduce intermediate velocities to separate the electric and magnetic forces completely. Substituting

$$\boldsymbol{v}_{t-\Delta t/2} = \boldsymbol{v}^- - \frac{e\boldsymbol{E}}{m}\frac{\Delta t}{2} \tag{8}$$

$$\boldsymbol{v}_{t+\Delta t/2} = \boldsymbol{v}^+ + \frac{e\boldsymbol{E}}{m}\frac{\Delta t}{2} \tag{9}$$

into Eqn. 7 yields an expression where $\boldsymbol{E}$ cancels entirely, leaving only a rotation due to $\boldsymbol{B}$:

$$\frac{\boldsymbol{v}^+ - \boldsymbol{v}^-}{\Delta t} = \frac{e}{2m}\left(\boldsymbol{v}^+ + \boldsymbol{v}^-\right) \times \boldsymbol{B} \tag{10}$$

For an efficient vector implementation define an intermediate vector $\boldsymbol{v'}$ bisecting $\boldsymbol{v}^+$ and $\boldsymbol{v}^-$ as

$$\boldsymbol{v'} = \boldsymbol{v}^- + \boldsymbol{v}^- \times \boldsymbol{t} \tag{11}$$

$$\boldsymbol{t} \equiv \frac{e\boldsymbol{B}}{m}\frac{\Delta t}{2} \tag{12}$$

where $\boldsymbol{t}$ is a vector representing the electron velocity vector's rotation due to the magnetic field in a half-timestep by angle $\omega_c \Delta t/2$. Then

$$\boldsymbol{v}^+ = \boldsymbol{v}^- + \boldsymbol{v}' \times \boldsymbol{s} \tag{13}$$

$$\boldsymbol{s} \equiv \frac{2\boldsymbol{t}}{1+t^2} \tag{14}$$

The leapfrog method in general is not self-starting, and given an initial condition $\boldsymbol{r}_0$ and $\boldsymbol{v}_0$ a half-step backwards in $\boldsymbol{v}$ is needed to generate $\boldsymbol{v}_{-\Delta t/2}$ to kickstart the leapfrog process.

To resolve the cyclotron motion, the electron trajectory is calculated with an adaptive timestep based on the local cyclotron frequency such that $\omega_c \Delta t \ll 1$. Choosing a timestep proportional to $1/\omega_c$ resolves trajectories well in high-field regions where the electron velocity vector rotates appreciably over short intervals without forcing a short, fixed maximum timestep across the entire simulation.

Boris' algorithm is sometimes called a drift-kick algorithm, since the electron is first accelerated in a linear "drift" by $\boldsymbol{E}$ only, and then the velocity vector is "kicked" or rotated by $\boldsymbol{B}$ between leapfrog iterations. The kick conserves energy to machine precision, so the main difficulty for energy conservation using the Boris algorithm is in regions of highly nonuniform $\boldsymbol{E}$. No maximum timestep is implemented in MCHall, but a maximum step size is enforced to prevent electrons from nonphysically gaining energy by "accelerating" due to a high electric field over a distance longer than that field is valid. This is particularly of concern for secondary electrons born with zero velocity in strong electric field regions with low B – as, for example, downstream on thruster centerline. A simple predictor / corrector scheme enforces the maximum step size by comparing the timestep and velocity magnitude after each Boris $\boldsymbol{v} \times \boldsymbol{B}$ integration. When the step size is too large, the timestep is reduced and, in the case of the corrector step, the timestep is resimulated.

For the special case in the H6 of a center-mount cathode and axisymmetric fields, a 2D simulation could suffice. Since the cathode centerline and thruster centerline coincide in this arrangement, it is possible to specify all thruster field properties ($\boldsymbol{E}$, $\boldsymbol{B}$ and n_n) independently of the azimuthal angle θ. However, MCHall is constructed in 3D to permit flexibility in introducing azimuthal perturbations on the axisymmetric fields at a later date.

1. Alternate integrators

In addition to the Boris method described above, we have also experimented with solving the implicit equations in Eqn. 7 directly via matrix algebra and also using a powerful embedded Runge-Kutta algorithm of 4th-5th order with adaptive timestep calculations. Both methods achieved similar or worse accuracy than the Boris algorithm, and with longer simulation times. Other methods such as Adams-Bashforth have been examined by Smith, who found them wanting.

Nevertheless, it may be possible to improve upon the Boris particle integration technique to increase simulation timestep durations (and thus speed) while maintaining conservation of energy. Equations of motion are a special class of differential equation that identically conserve the Hamiltonian of the motion. For charged particles in electromagnetic fields, the Hamiltonian H is defined as:

$$H = \frac{1}{2m}(\boldsymbol{p} + e\boldsymbol{A})^2 - e\Phi$$

Such conserved quantities enable a special class of numerical integrators called symplectic algorithms that maintain a bounded error in the conserved quantity (here, total energy) independent of simulation time or number of timesteps. Another option for charged particle trajectory integration is the semi-analytic technique of Biagi, used in electron swarm tracking in gas avalanche radiation detectors.[38]

Ultimately the field of charged particle trajectory integration is widely applicable, and while the electric propulsion community has only recently begun to attempt such simulations, a more detailed review of similar work in neighboring fields is recommended though unfortunately beyond the scope of this work. The challenging field configuration of the Hall thruster, with prominent magnetic mirroring, high field gradients and long electron confinement times make it a difficult configuration to numerically integrate accurately, and improved methods of numerical integration are always welcome.

B. Simulation Domain and Experimental Fields

The simulation domain extends 1.75 thruster mean channel radii in the radial direction and 2.6 radii in the axial direction. The electric field is prescribed by plasma potential measurements from Jameson in the JPL copy of the H6 using floating emissive probes corrected for electron temperature.[34] The magnetic field is obtained from a finite element simulation in Infolytica's commercial MagNet software package. The neutral density is also from Jameson, using relative densities obtained via optical measurements and scaled to absolute values using neutral density estimates from HPHall.

The magnetic field simulation takes into account only the vacuum field configuration, neglecting any self-fields caused by the currents within the plasma during operation. Both the electric and magnetic field are imported into the simulation on a 1 mm mesh; the electric field is interpolated to this resolution before importing and the magnetic field is directly calculated in MagNet at this level. On each timestep the local fields at the electron position are bilinearly interpolated from the values at each corner of the current mesh cell.

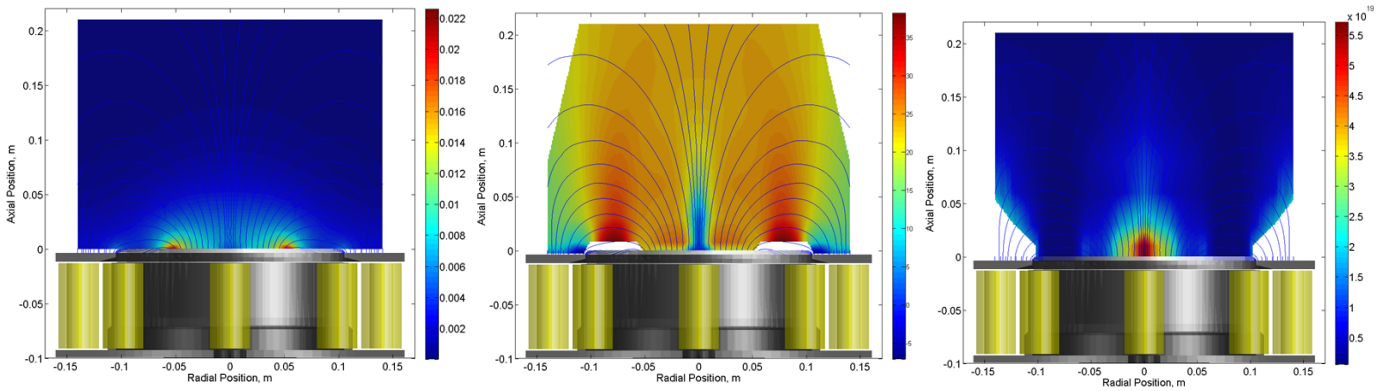

Figure 1. MCHall Input Field Meshes. Left to right, the magnetic field strength $|B|$ [Tesla], the plasma potential V_p [V] and the neutral density n_n [m^{-3}]. Magnetic field streamlines are overlaid on all meshes.

Since Jameson's data extends only to approximately a centimeter in front of the thruster face; the very near-field and sheath have been addressed with flush-mounted planar Langmuir probes mounted within 3 mm of the front poles of the H6, nearly level with the thruster exit plane. These probes resolve the plasma potential, density and electron temperature in the very near field. Assuming the electron temperature and density to be characteristic of the thruster sheath, the sheath thickness is at most 0.3 mm thick in this region and is effectively treated as a perfectly thin barrier with potential equal to the difference between the plasma potential measured at the probes and the grounded thruster pole pieces.

C. Electron Sourcing

MCHall treats the cathode as an electron point source fully characterized by an electron energy distribution function (EEDF) and a spatial ejection angle distribution. Goebel has characterized a lanthanum hexaboride (LaB6) hollow cathode similar to the one used in the H6 Hall thruster, measuring an electron temperature of approximately 2 eV at the cathode orifice during a 25-amp operating condition at 10 sccm, similar to the 20-amp 7 sccm nominal operating condition for the H6 hollow cathode.[35] Based on this measurement MCHall seeds electrons from the cathode orifice with a Maxwellian energy distribution about temperature 2 eV. The EEDF is divided into discrete bins and each bin is further segmented into a predetermined spatial distribution of emission angles for the velocity vector. Energy isotropy is explicitly assumed since the same EEDF is distributed across all emission angles.

The distribution of velocity vectors in MCHall is not strictly half-Maxwellian, i.e., uniformly distributed over a hemisphere of solid angle. Lacking experimental data on the cathode electron emission angle, we make an educated guess that electrons are sourced into the half-space $z > 0$ from the cathode orifice at the origin according to a Gaussian distribution of angles with respect to thruster centerline and uniformly in the azimuth (Figure 2). This attempts to account for the likely focusing of the electron current into a directed beam by the axial magnetic field. For the polar angle from centerline ϕ and azimuthal angle θ the distribution function is then

$$f(\phi, \theta) = Ae^{-\phi^2/2\sigma_\phi^2}$$

where σ_ϕ is the standard deviation, taken here to be 30 degrees, of polar emission angle and A is a normalizing factor. The choice of 30 degrees is largely an arbitrary one; it is also the angle used by Smith. The number of electrons sourced into an element of solid angle $\phi\, d\phi\, d\theta$ is:

$$N = f(\phi, \theta)\phi\, d\phi\, d\theta$$

The integration over θ is trivial and the expression for N may be further simplified as

$$N = F(\phi)d\phi = B\phi e^{-\phi^2/2\sigma_\phi^2} d\phi$$

where B is a new normalizing factor and the function $F(\phi)$ is the distribution over the polar angle ϕ alone.

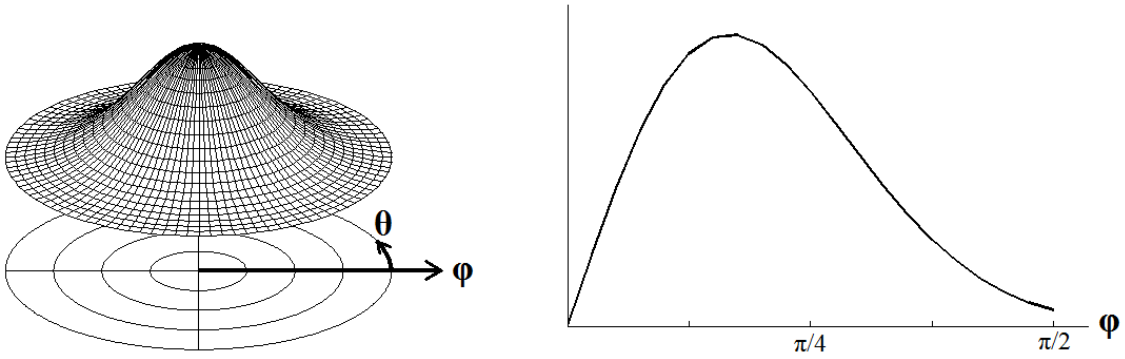

Figure 2. Left, the assumed Gaussian distribution function $f(\phi, \theta)$ of the cathode electron emission angle; right, the integrated distribution function $F(\phi)$ of the polar angle alone.

D. Collisional Electron Scattering

The electron collision frequency ν depends on the collision cross-section σ, the incident electron velocity v and the background species density n. Only electron-neutral collisions are presently considered. This is a shortcoming of MCHall since the electron-ion collision frequency probably exceeds the electron-neutral frequency in the main ion beam in front of the discharge channel, but full maps of the plasma density in this region are not expected until later in 2011.

Cross-sections are drawn from the Electron Impact Processes Hybrid Plasma Equipment Model (HPEM) code maintained by Professor Mark Kushner at the University of Michigan Department of Electrical Engineering and Computer Science.[39] Cross-sections with ions are available from this code as well, and will be implemented once plasma density maps become available. Cross-sections with excited neutral states are not planned for inclusion due to the difficulty of obtaining relative density measurements of excited states in the plume.

Given these three quantities, the collision frequency for a particle at constant velocity in a uniform background density is

$$\nu = n\sigma v \tag{15}$$

For realistic variable density, particle velocity, and cross section $\sigma = \sigma(T_e)$, this expression is valid only for small time intervals Δt during which the quantities n and v can be assumed constant. Generally this interval is sufficiently short that $\nu\Delta t \ll 1$, so in any given timestep a collision is unexpected, but over several such steps the likelihood of a collision event "builds up" until eventually a collision is due to take place. This scenario is well-suited to Monte Carlo methods, where by treating a sufficiently large number of statistically independent trials the probable final outcome(s) of a series of random events can be estimated. In MCHall likely electron transport pathways are estimated by simulating a large number of electron trajectories through random scattering processes with an appropriate distribution of initial conditions. Whether a number of trials is "sufficiently large" is a matter of convergence of the model's final state; for MCHall, we treat the model as converged when doubling the number of particles does not appreciably affect the results.

Detailed implementation of a Monte Carlo scattering process is outlined in the review paper by Birdsall.[40] The probability of a particle collision in a time step Δt is

$$P_{collision} = 1 - exp(-\nu \Delta t) \tag{16}$$

For the timesteps and conditions in MCHall the argument of the exponent is very small and Eqn. (16) may be approximated by Taylor expansion of the exponent as

$$P_{collision} \approx \nu \Delta t \tag{17}$$

The "building up" of probability over time occurs by repeatedly comparing the collision probability with a unique random number R_1 generated on each timestep. If $P > R_1$, a collision occurs. In practice, several collision pathways are considered simultaneously, and the cross-section used to calculate ν in Eqn. (15) is a total cross section computed as the sum of the cross sections for each event. If a collision occurs on a given timestep, a second random number R_2 is generated, the relative cross-sections are lined up on the range from 0 to 1 as σ_1/σ_{tot}, $(\sigma_1 + \sigma_2)/\sigma_{tot}$, $(\sigma_1 + \sigma_2 + \sigma_3)/\sigma_{tot}$, etc., and the reaction is given by the scattering process covering the range where R_2 falls. To ensure statistical independence, each electron is assigned a unique seed in the random number generator.

After a collision MCHall chooses a new unit vector direction distributed randomly over the unit sphere and, after adjusting the electron energy to account for any losses in the scattering process (for example, -12.13 eV for ionization), the electron is sent along its way in the new direction.

In MCHall secondary electrons from ionization are registered as they are created and subsequently tracked in addition to the primary electrons from the cathode. This implementation is recursive, such that secondary electrons can create and register tertiary electrons, and so on. Secondary electrons are seeded at rest from the position of the ionizing collision. Secondary electron tracking is important because, given the 80% / 20% plume/channel split of cathode-born electrons in the H6, to maintain the discharge current each channel-bound electron in the 20% must generate, on average, 4 new channel-bound electrons either directly by ionization or indirectly through its ionization-born descendants. While much of that ionization may occur in the discharge channel, some may occur in the near field as well, and since the secondary electrons get "free passage" across the magnetic field from the cathode to their birthplace they should not be overlooked.

E. Simulation parallelization and speed

The code is run in parallel on an AMD Opteron 6128 8-core 2 GHz processor in MATLAB r2011a. The baseline simulations presented in this work of approximately 10^4 electrons require about 2 hours, for an average simulation rate of about 6 seconds / electron / core. The low simulation speed is due to the very small timesteps, $\omega_c \Delta t = 10^{-3}$, used to ensure conservation of energy during confined electron orbits which may have durations up to 10^{-4}seconds, corresponding to up to several million timesteps. An arbitrary cutoff was imposed at 10^{-4} seconds for this simulation, since this corresponds to the period of a 10 kHz oscillation, on the order of the breathing mode, and conclusions drawn from static field simulations at timescales longer than this are considered questionable.

Parallelization of the code is accomplished by first binning the EEDF into a suitable number of discrete energy levels to adequately characterize the EEDF and then, for each discrete energy level, seeding a complete spatial distribution of electrons into $F(\phi)$ at that energy with randomly assigned azimuthal emission angles θ. Different energy level bins are simulated in parallel, while spatial bins are simulated in series within each energy. In the baseline simulations of this work 100 energy levels of 100 electrons each are simulated, for a total of approximately 10^4 electrons, plus any secondary electrons.

For a given timestep, field interpolation is the largest part of simulation time, taking about 50% of a given simulation run, while the Boris algorithm is quite compact and takes only about 20%. Speed gains are obtained by defining electric, magnetic and neutral density fields on a uniform mesh and doing only one interpolation step for all three quantities. Only the electric and magnetic fields are bilinearly interpolated; the neutral density and plasma potential are chosen as the nearest neighbor in the grid. Plasma potential is only tracked to check energy conservation over the course of a run.

IV. Simulation Results

The baseline MCHall simulation is of 10^4 electrons seeded into the H6 plume from a point source cathode on thruster centerline at the exit plane. There are few surprises in the baseline; given that classical transport is not

expected to move electrons across field lines well if at all, the baseline behaves as expected in delivering almost all electrons to an axisymmetric focused dispersal into the far-field simulation boundary within a fraction of a microsecond. The mean electron lifetime is 1.1×10^{-7} seconds. A small fraction of electrons, less than 5% of the total, are reflected back into the cathode orifice or into a collision with the cathode keeper surface due to a weak magnetic mirror in front of the cathode orifice. Two electron trajectories are shown in Figure 3, one a typical case of an electron emitted from the cathode and departing without interruption to the far field plume, the other a very atypical case of a long-lived secondary electron confined for an extended azimuthal drift. The typical electron has a lifetime of only a fraction of a microsecond, experiences no collisions, and exits the simulation domain downstream in a narrowly confined region close to the thruster and cathode centerline axis.

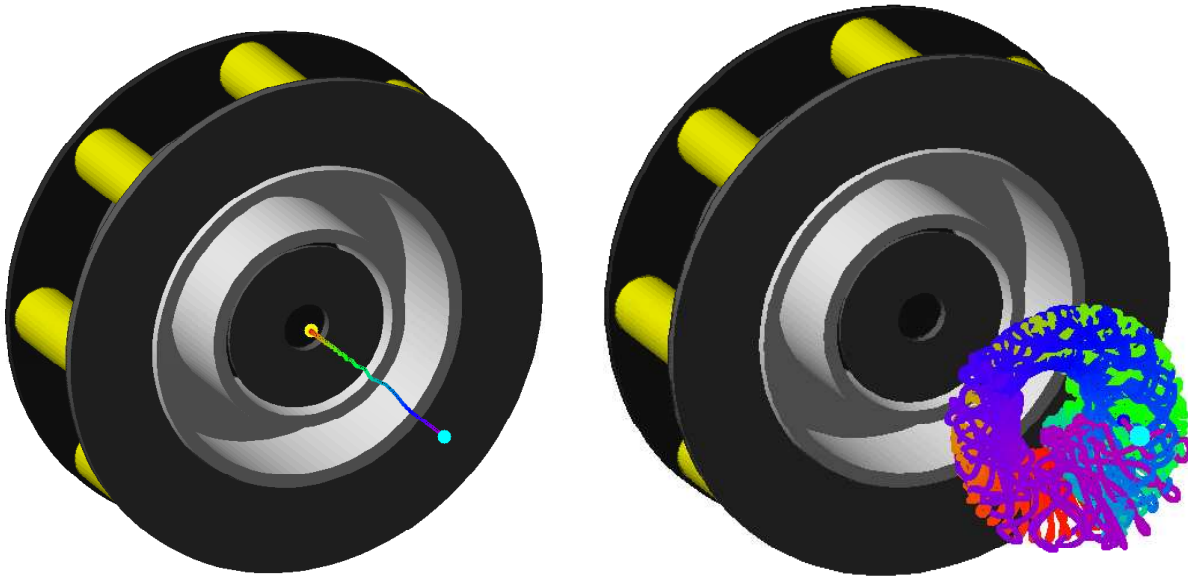

Figure 3. Two electron orbits observed out of over 10^4 in a simulation run of MCHall. Left, a typical orbit with a lifetime on the order of 10^{-7} seconds stays confined to thruster centerline after being emitted from a centrally mounted cathode (not pictured). The orbit is color-coded in time from red to violet, the yellow dot marks the sourcing point, and the blue dot marks the exit from the simulation domain. At right, an atypical secondary electron generated by an ionizing collision in the near-field is held in a confined azimuthal drift on the order of 10^{-4} seconds. This orbit is the longest-lived electron in the simulation run.

While some 80% of all electrons that should depart into the far field to neutralize the beam current, it is remarkable that of over ten thousand electrons seeded into the thruster plume, not one in this simulation through the static experimental fields reaches the channel entrance. This is in rather severe contrast to the simulations with an external cathode of Smith, who arrived at a conclusion of substantial transport due to thruster surface collisions in time-averaged fields generated from hybrid-PIC simulations. This model certainly shows that this is not the case for the centrally mounted cathode. In Smith's work the cathode's orientation initially directed electrons into the magnetic mirror over the inner pole, while the central cathode in the H6 seeds electrons from as deep as it is possible to go in that mirror. The initial electron velocities are such that the electrons tightly follow the magnetic field on thruster centerline into the far field, exiting the simulation domain an average of 6.5 mm of centerline at 2.6 mean thruster channel radii axially downstream, with 50% of all electrons exiting within a median 3 mm from centerline. Again, while the work of Smith found little contribution to cross-field transport due to binary plume collisions with neutrals, collisional scattering is the only reason that a few electrons are knocked off this highway to the far field to form the long-lived tail of the distribution of lifetimes in Figure 4.

The majority of electron lifetimes in the plume are distributed by the travel time from the cathode to exit plane given by the Maxwellian velocity distribution and accounting for the strong axial electric fields near thruster centerline. One interesting result of this work is the inclusion of secondary electrons, which when broken out account disproportionately for the long tail of the lifetime distribution. Part of this is because of the zero energy these secondaries are seeded with, but part is because with zero initial velocity they are free to become trapped on the magnetic field lines where they are born in a drift pattern and enter into extended, confined orbits. Of the handful of electrons in the baseline simulation with lifetimes longer than a microsecond, all are secondary electrons. The spike in population

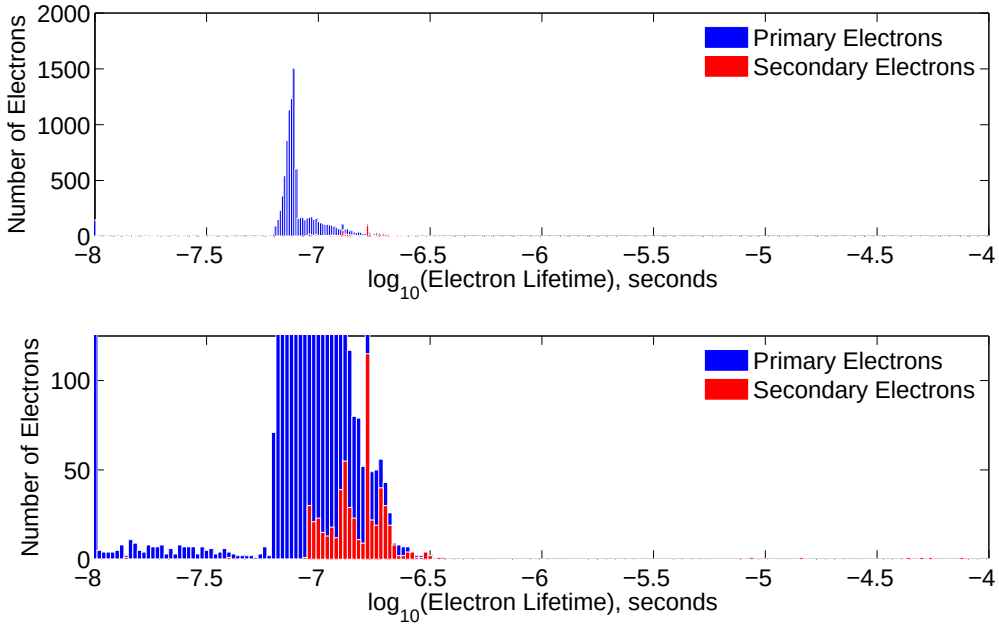

Figure 4. Distribution of electron lifetimes seeded at 2 eV from the centrally mounted H6 cathode. Above, the entire distribution is shown, while below the scale is exaggerated to show the contributions of secondary electrons from ionization events. The mean lifetime over all electrons is 1.1×10^{-7} seconds. The secondary electrons, shown in red, have a longer average lifetime than primaries since they are born at zero velocity and tend to be born off thruster centerline, where they are more likely to be caught in an azimuthal $E \times B$ drift before exiting the simulation. The very long-lived tail of the distribution is entirely composed of secondary electrons.

at 10^{-8} seconds is an aggregate of all electrons having very short lifetimes $\tau < 10^{-8}$.

In terms of proportional representation in the lifetime distribution, note that in a real discharge electrons are continuously seeded from the cathode, so long-lived electron populations observed in isolated seeding like that shown here would be more strongly represented at steady state from continual seeding in a normalized distribution. This scaling would be by a factor equal to their lifetime divided by the lifetime of the mean of the distribution. For the case here of electrons with lifetimes near to 10^{-4} seconds in a distribution with mean on the order of 10^{-7} seconds, these small populations would be a thousand times more prevalent at steady state. This is compelling motivation to resolve these long-lived tails better in future simulations, which given the large number of required timesteps further drives the search for improved numerical integration techniques. Conversely, the short-lived tail of electrons with lifetimes below 10^{-8} seconds are less prevalent in a steady state distribution and not as worthy of notice.

V. Conclusions

An electron trajectory integration model, MCHall, has been developed for large-scale simulation of electron transport in static and eventually time-resolved Hall thruster fields. The code records electron lifetimes and ultimate destinations in the plume, and accounts for the generation of secondary electrons by ionizing collisions of neutral atoms using Monte Carlo methods. A baseline demonstration simulation of classical transport in static thruster fields reveals that, out of over ten thousand electrons seeded from a centrally mounted cathode into the thruster plume, not one makes it to the discharge channel, or even to contact with the inner or outer magnet poles.

While the MCHall baseline simulation is illustrative of the types of orbits and drifts that cathode-born electrons experience, we do not conclude at this time that collisional transport does not exist in the plume for centrally mounted cathodes or even that it is not significant. The limitations of the static field assumption mean that in the real device, where time-varying fields are certainly present, vastly different physics may be capable of substantially impacting electron transport. What is reasonable to conclude is that, within the framework of a static field configuration, classical drift orbits are insufficient to drive reasonable cross-field electron current to sustain a discharge, even with binary collisions and thruster surface interactions included. This is as much a statement about the poor validity of a static

field assumption in a Hall thruster discharge as it is about the viability or level of collisional cross-field transport in the near-field, and motivates the prompt acquisition of time-resolved data for inclusion in the model.

Acknowledgments

The authors thank Drs. Richard Hofer and Dan Goebel of the Jet Propulsion Laboratory for access to plasma potential measurements obtained by Dr. Kristina Jameson on the JPL copy of the H6 Hall thruster. The simulations in this paper would not have been possible without computing resources funded by a Strategic University Research Partnership (SURP) with the Jet Propulsion Laboratory under principal investigator Dr. Richard Hofer. The first author is grateful for the support of the National Science Foundation Graduate Research Fellowship Program, as well as the Tau Beta Pi Foundation and the National Defense Industry Association. The authors also thank Dr. Andrew Smith, now of Lawrence Livermore National Laboratory, for fruitful discussions on large-scale electron trajectory integration.

References

[1]Huang, W., *David's Thesis, title to be filled in*, Ph.D. thesis, University of Michigan, Ann Arbor, MI, 2011.

[2]Brophy, J., Gershman, R., Strange, N., Landau, D., Merrill, R., and Kerslake, T., "300-kW Solar Electric Propulsion System Configuration for Human Exploration of Near-Earth Asteroids," July 2011.

[3]Kamhawi, H., Haag, T., Jacobson, D., and Manzella, D., "Performance Evaluation of the NASA-300M 20 kW Hall Thruster," July 2011.

[4]Jacobson, D., Manzella, D., Hofer, R., and Peterson, P., "NASA's 2004 Hall Thruster Program," July 2004.

[5]Jankovsky, R., Jacobson, D., Sarmiento, C., Pinero, L., Manzella, D., Hofer, R., and Peterson, P., "NASA's Hall Thruster Program 2002," July 2002.

[6]Szabo, J., Pote, B., Hruby, V., Byrne, L., Tadrake, R., Kolencik, G., Kamhawi, H., and Haag, T., "A Commercial One Newton Hall Effect Thruster for High Power In-Space Missions," July 2011.

[7]Florenz, R. F. and Gallimore, A. D., "Developmental Status of a 100-kW Class Laboratory Nested channel Hall Thruster," *32nd International Electric Propulsion Conference*, IEPC-2011-246, Wiesbaden, Germany, 2011.

[8]Liang, R. and Gallimore, A., "Far-Field Plume Measurements of a Nested-Channel Hall-Effect Thruster," *49th AIAA Aerospace Sciences Meeting*, AIAA-2011-1016, Jan. 2011.

[9]Janes, G. S. and Lowder, R. S., "Anomalous Electron Diffusion and Ion Acceleration in a Low-Density Plasma," *Physics of Fluids*, Vol. 9, 1966, pp. 1115.

[10]Morozov, A. I., "Wall conduction in a highly magnetized plasma," *Journal of Applied Mechanics and Technical Physics*, Vol. 9, No. 3, 1968, pp. 249–251.

[11]Morozov, A. I., Esinchuk, Y. V., Tilinin, G. N., Trofimov, A. V., Sharov, Y. A., and Shchepkin, G. Y., "Plasma Accelerator with Closed Electron Drift and Extended Acceleration Zone," *Soviet Physics Technical Physics*, Vol. 17, July 1972, pp. 38.

[12]Smith, A. W. and Cappelli, M. A., "Single particle simulations of electron transport in the near-field of Hall thrusters," *Journal of Physics D: Applied Physics*, Vol. 43, No. 4, 2010, pp. 045203.

[13]Fife, J. M., *Hybrid-PIC Modeling and Electrostatic Probe Survey of Hall Thrusters*, Ph.D. thesis, Massachusetts Institute of Technology, Cambridge, MA, 1998.

[14]Fife, J. M., Martinez-Sanchez, M., and Szabo, J., "A numerical study of low-frequency discharge oscillations in Hall thrusters," *33rd AIAA/ASME/SAE/ASEE Joint Propulsion Conference & Exhibit, Seattle, WA*, 1997.

[15]Boeuf, J. P. and Garrigues, L., "Low frequency oscillations in a stationary plasma thruster," *Journal of Applied Physics*, Vol. 84, No. 7, Oct. 1998, pp. 3541–3554.

[16]Bohm, D., Burhop, E. H. S., and Massey, H. S. W., "The Use of Probes for Plasma Exploration in Strong Magnetic Fields," *The Characteristics of Electrical Discharges in Magnetic Fields*, edited by A. Guthrie and R. Wakerling, McGraw-Hill, 1949.

[17]Hagelaar, G. J. M., Bareilles, J., Garrigues, L., and Boeuf, J. P., "Two-dimensional model of a stationary plasma thruster," *Journal of Applied Physics*, Vol. 91, No. 9, 2002, pp. 5592.

[18]Koo, J. W. and Boyd, I. D., "Modeling of anomalous electron mobility in Hall thrusters," *Physics of Plasmas*, Vol. 13, No. 3, March 2006, pp. 033501–7.

[19]Hofer, R. R., Katz, I., Mikellides, I. G., Goebel, D. M., Jameson, K. K., Sullivan, R. M., and Johnson, L. K., "Efficacy of Electron Mobility Models in Hybrid-PIC Hall Thruster Simulations," 44th AIAA/ASME/SAE/ASEE Joint Propulsion Conference, Hartford, CT, AIAA-2008-4924, 2008.

[20]Fernandez, E., Knoll, A., and Cappelli, M. A., "An axial-azimuthal hybrid simulation of coaxial Hall thrusters," *42nd AIAA/ASME/SAE/ASEE Joint Propulsion Conference & Exhibit*, AIAA 2006-4329, 2006.

[21]Adam, J. C., Héron, A., and Laval, G., "Study of stationary plasma thrusters using two-dimensional fully kinetic simulations," *Physics of Plasmas*, Vol. 11, 2004, pp. 295.

[22]Adam, J. C., Boeuf, J. P., Dubuit, N., Dudeck, M., Garrigues, L., Gresillon, D., Heron, A., Hagelaar, G. J. M., Kulaev, V., Lemoine, N., Mazouffre, S., Perez Luna, J., Pisarev, V., and Tsikata, S., "Physics, simulation and diagnostics of Hall effect thrusters," *Plasma Physics and Controlled Fusion*, Vol. 50, Dec. 2008, pp. 4041.

[23]Smith, A. W. and Cappelli, M. A., "Investigation of field structure and electron behavior in near-field of Hall thrusters," 42nd AIAA/ASME/SAE/ASEE Joint Propulsion Conference and Exhibit, Sacramento, CA, AIAA 2006-4835, 2006.

[24]Smith, A. W. and Cappelli, M. A., "Numerical investigation of electron behavior in the near-field of Hall thrusters," 43rd AIAA/ASME/SAE/ASEE Joint Propulsion Conference & Exhibit, Cincinnati, OH, AIAA 2007-5240, 2007.

[25]Alman, D. A., Rovey, J. L., Stubbers, R. A., and Jurczyk, B. E., "Hall Thruster Electron Mobility Investigation using Full 3D Monte Carlo Trajectory Simulations," *30th International Electric Propulsion Conference*, IEPC 2007-291, 2007.

[26]Lobbia, R. B. and Gallimore, A. D., "Temporal limits of a rapidly swept Langmuir probe," *Physics of Plasmas*, Vol. 17, No. 7, 2010, pp. 073502.

[27]Lobbia, R. B. and Gallimore, A. D., "High-speed dual Langmuir probe," *Review of Scientific Instruments*, Vol. 81, No. 7, 2010, pp. 073503.

[28]McDonald, M. S. and Gallimore, A. D., "Rotating Spoke Instabilities in Hall Thrusters," *IEEE Transactions on Plasma Science (to be published)*, 2011.

[29]McDonald, M. S. and Gallimore, A. D., "Measurement of Cross-Field Electron Current in a Hall Thruster Due to Rotating Spoke Instabilities," *47th AIAA/ASME/SAE/ASEE Joint Propulsion Conference & Exhibit*, AIAA 2011-5810, 2011.

[30]Reid, B. M. and Gallimore, A. D., "Langmuir Probe Measurements in the Discharge Channel of a 6-kW Hall Thruster," *44th AIAA/ASME/SAE/ASEE Joint Propulsion Conference & Exhibit*, AIAA 2008-4920, 2008.

[31]Reid, B. M. and Gallimore, A. D., "Plasma Potential Measurements in the Discharge Channel of a 6-kW Hall Thruster," *44th AIAA/ASME/SAE/ASEE Joint Propulsion Conference & Exhibit*, AIAA 2008-5185, 2008.

[32]Reid, B., *The Influence of Neutral Flow Rate in the Operation of Hall Thrusters*, Ph.D. thesis, University of Michigan, Ann Arbor, MI, 2009.

[33]Mikellides, I. G., Katz, I., and Hofer, R. R., "Design of a Laboratory Hall Thruster with Magnetically Shielded Channel Walls, Phase I: Numerical Simulations," *47th AIAA/ASME/SAE/ASEE Joint Propulsion Conference & Exhibit*, AIAA 2011-5809, 2011.

[34]Jameson, K., *Investigation of Hollow Cathode Effects on Total Thruster Efficiency in a 6-kW Hall Thruster*, Ph.D. thesis, University of California Los Angeles, Los Angeles, CA, 2008.

[35]Goebel, D. M., Jameson, K. K., Watkins, R. M., and Katz, I., "Hollow cathode and keeper-region plasma measurements using ultra-fast miniature scanning probes," *40th AIAA/ASME/SAE/ASEE Joint Propulsion Conference & Exhibit*, AIAA 2004-3430, 2004.

[36]Birdsall, C. K. and Langdon, A. B., *Plasma physics via computer simulation*, IOP Publishing Ltd., Bristol, England, 2004.

[37]"Smith and Cappelli - 2006 - Investigation of field structure and electron beha.pdf," .

[38]Biagi, S. F., "Monte Carlo simulation of electron drift and diffusion in counting gases under the influence of electric and magnetic fields," *Nuclear Instruments and Methods in Physics Research Section A: Accelerators, Spectrometers, Detectors and Associated Equipment*, Vol. 421, No. 1-2, Jan. 1999, pp. 234–240.

[39]Kushner, M., "Computational Plasma Science and Engineering Group HPEM Database," 2010.

[40]Birdsall, C. K., "Particle-in-cell charged-particle simulations, plus Monte Carlo collisions with neutral atoms, PIC-MCC," *IEEE Transactions on Plasma Science*, Vol. 19, No. 2, 1991, pp. 65–85.